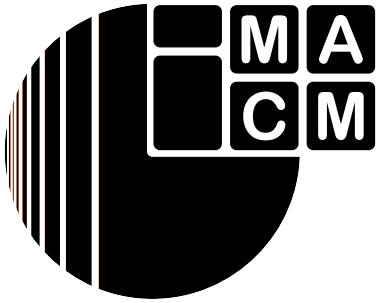


Bergische Universität Wuppertal

Fachbereich Mathematik und Naturwissenschaften

Institute of Mathematical Modelling, Analysis and Computational Mathematics
(IMACM)

Preprint BUW-IMACM 18/14

Jan Kühn, Andreas Bartel and Piotr Putek

# A Thermal Extension of Tellinen's Scalar Hysteresis Model

October 15, 2018

http://www.math.uni-wuppertal.de

# A Thermal Extension of Tellinen's Scalar Hysteresis Model

Jan Kühn Andreas Bartel Piotr Putek

October 15, 2018

There exist different models which approximate the phenomenon of magnetic hysteresis. But only some of them consider a thermal dependency initially or were extended in this respect. In the following, Tellinen's scalar magnetic hysteresis model is reviewed and illustrated. In the process, special focus is laid upon the ideas and physical motivation. Afterwards, the underlying concept is adapted and extended w.r.t a thermal behavior. In the end, a temperature dependent scalar magnetic hysteresis model is deduced and investigated.

## 1 Introduction and Motivation

In many applications, ferromagnetic materials are exposed to a broad range of temperatures. In extreme cases the temperature approaches or exceeds the Curie point. Then, the material is losing its ferromagnetic properties and transits to a paramagnetic state. But even for less significant temperature changes, the magnetic properties are affected. This has been and is still being researched [1, 6]. By now, several magnetic hysteresis models exist, e.g., [5, 7–9]. However, only some of them originally incorporated thermal influence or were extended to do so (e.g. [2, 3]). To our knowledge Tellinen's model [5] has not been one of them. We have chosen Tellinen's model because it is easy to understand, simple to implement and overall fast to compute. Nevertheless, it is still competitive in comparison to more complicated models [4]. Tellinen's model is motivated by phenomenological observations and can be more or less graphically described. It is very adaptable w.r.t. the input parameters. We will derive an extended model, such that it includes temperature dependence, while retaining the above mentioned positive properties. The following sections are organized as follows: First, the original model is introduced and the approaches used are presented. The thermal extension is then modelled on the basis of the same approaches. Afterwards, the necessary steps for embedding in a magnetic field simulation are shown.

## 2 Tellinen's Hysteresis Model

Originally, this model was defined in [5]. In order to prepare the thermal extension, we summarize core modeling issues.

**Input data.** We assume a magnetically fully saturated material, let say $h, b \ll 0$ with scalar magnetic flux density $b$ and field strength $h$. Then, the transition to the saturated state of opposite polarity, $h, b \gg 0$, results in a material specific function $b = B^+_{\mathrm{sat}}(h)$ (for a monotone transition from $h \ll 0$ to $h \gg 0$). It is called the saturation or limiting curve. For $B^+_{\mathrm{sat}}$ to be a valid input for Tellinen's model, a few constraints must be fulfilled. Firstly, since both magnetic polarization directions are interchangeable, there must exist an analogous function for the transition from $h \gg 0$ to $h \ll 0$, say $B^-_{\mathrm{sat}}(h)$. It can be defined by symmetry, i.e.,

$$B^-_{\mathrm{sat}}(h) := -B^+_{\mathrm{sat}}(-h)\,. \tag{1}$$

Physically, $B^-_{\mathrm{sat}}$ must lie above $B^+_{\mathrm{sat}}$, such that eventually a loop is formed, i.e.,

$$B^+_{\mathrm{sat}}(h) < B^-_{\mathrm{sat}}(h), \qquad \lim_{|h|\to\infty} \left(B^-_{\mathrm{sat}}(h) - B^+_{\mathrm{sat}}(h)\right) = 0, \tag{2}$$

see Fig. 1. Secondly, $B^+_{\mathrm{sat}}$ must be differentiable ($C^1$) with bounds from below on

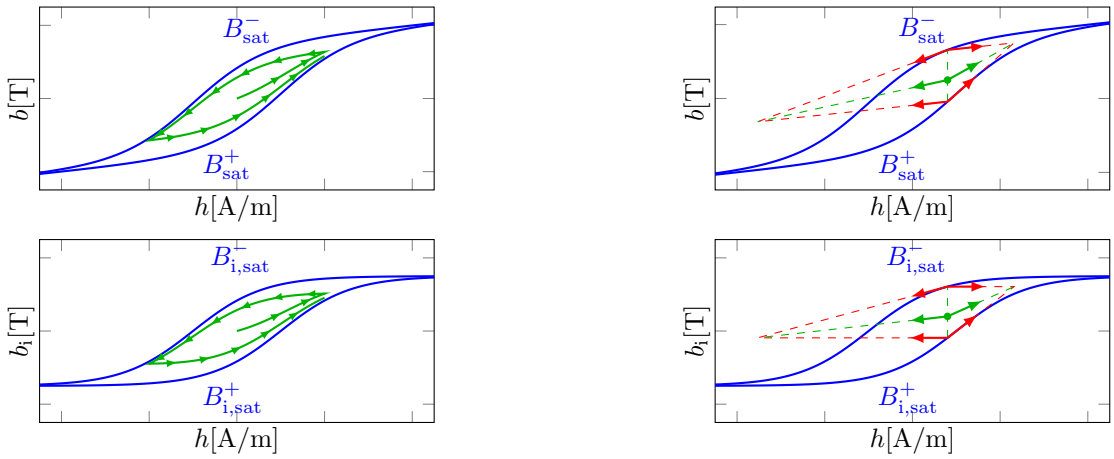


Figure 1: The first row represents $b/h$-curves, while the second row gives $b_{\mathrm{i}}/h$-curves for intrinsic induction. The left column depicts a sample hysteresis loop starting from the origin. The right column shows the idea of Tellinen's model. For a given working point $(h, b)$ the resulting slope $\mu_{\mathrm{diff}}$ is depicted (inner arrows), depending on increasing or decreasing field strength.

the derivative by $\mu_0$ (permeability of vacuum):

$$\frac{d}{dh} B^+_{\mathrm{sat}}(h) \geq \mu_0 > 0\,, \qquad \lim_{|h|\to\infty} \frac{d}{dh} B^+_{\mathrm{sat}}(h) = \mu_0\,. \tag{3}$$

Due to (3), this yields a model for ferromagnetic and paramagnetic materials. In the further course, let the given $B^{\pm}_{\mathrm{sat}}$ satisfy the constraints above.

**Realization and physical motivation.** Tellinen's model is based upon two major principles. Firstly, the derivative $\frac{db}{dh}$ for the current working point $(h,b)$ is calculated depending on whether $h$ is de- or increased. This reflects the fact that hysteresis is not reversible. Secondly, values for the derivative $\frac{db}{dh}$ are fixed on both boundaries $B^{+}_{\mathrm{sat}}$ and $B^{-}_{\mathrm{sat}}$ and linear interpolation is used for intermediate values. The choice of the boundary values is physically motivated and derived also from input data.

To define Tellinen's model, we introduce the set of all valid states $I$ within the boundaries $B^{+}_{\mathrm{sat}}$ and $B^{-}_{\mathrm{sat}}$ by

$$I := \left\{ (h,b) \in \mathbb{R}^2 \;\middle|\; B^{+}_{\mathrm{sat}}(h) \leq b \leq B^{-}_{\mathrm{sat}}(h) \right\}. \tag{4}$$

For any $(h,b) \in I$, the relative (vertical) position between the boundaries $B^{+}_{\mathrm{sat}}$ and $B^{-}_{\mathrm{sat}}$ can be calculated by

$$\lambda = \frac{B^{-}_{\mathrm{sat}}(h) - b}{B^{-}_{\mathrm{sat}}(h) - B^{+}_{\mathrm{sat}}(h)} \in [0,1]. \tag{5}$$

Now, combining assignments of $\frac{db}{dh}$ on the boundary, i.e., for $\lambda = 0$ and $\lambda = 1$ and linear interpolation, we obtain for the distinguished $dh < 0$ and $dh > 0$ cases [5]

$$\frac{db}{dh} = \begin{cases} \mu^{+}_{\mathrm{diff}} = \lambda \dfrac{dB^{+}_{\mathrm{sat}}(h)}{dh} + (1-\lambda)\mu_0 & \text{if } dh > 0\,, \\ \mu^{-}_{\mathrm{diff}} = \lambda \mu_0 + (1-\lambda)\dfrac{dB^{-}_{\mathrm{sat}}(h)}{dh} & \text{if } dh < 0\,. \end{cases} \tag{6}$$

Tellinen's model is fully defined by (5-6). By construction, an analytical solution, starting at $(h_0,b_0) \in I$, progressed by (6), always stays in $I$. To physically motivate (6), we delve further into the derivation [5]. To this end, we examine the intrinsic induction $b_{\mathrm{i}} := b(h) - \mu_0 h$. Here, the pure vacuum term $\mu_0 h$ is subtracted. On the boundary (saturation), we have

$$B^{\pm}_{\mathrm{i,sat}}(h) = B^{\pm}_{\mathrm{sat}}(h) - \mu_0 h\,, \qquad \frac{dB^{\pm}_{\mathrm{i,sat}}}{dh} = \frac{dB^{\pm}_{\mathrm{sat}}}{dh} - \mu_0\,. \tag{7}$$

All properties of $B^{\pm}_{\mathrm{sat}}$ and $\frac{dB^{\pm}_{\mathrm{sat}}}{dh}$ can easily be transferred to $B^{\pm}_{\mathrm{i,sat}}$ and $\frac{dB^{\pm}_{\mathrm{i,sat}}}{dh}$, see Fig. 1. In [5], it is argued that a saturated material, i.e., $b_{\mathrm{i}} = B^{+}_{\mathrm{i,sat}}(h)$ or $b_{\mathrm{i}} = B^{-}_{\mathrm{i,sat}}(h)$, resists a magnetization of opposing polarization. Thus, if the material is in the state $(h, b_{\mathrm{i}})$ with $b_{\mathrm{i}} = B^{+}_{\mathrm{i,sat}}(h)$, we model $\frac{db_{\mathrm{i}}}{dh} = \frac{dB^{+}_{\mathrm{i,sat}}}{dh}$ for $dh > 0$, because this has been measured by $B^{+}_{\mathrm{i,sat}}$. But for $dh < 0$, we explicitly set $\frac{db_{\mathrm{i}}}{dh} = 0$, because the material opposes the magnetization, and therefore, does not contribute to $b_{\mathrm{i}}$. The analogous approach is used for $b_{\mathrm{i}} = B^{-}_{\mathrm{i,sat}}(h)$. Together with (7) this results in (6).

**Implementation details and drawbacks.** The implementation of Tellinen's model is easy, but the integration into a simulation tool, e.g., based on finite elements, has to be done carefully. For a critical discussion, we mention two details:

a) A priori in a time step, it is unknown if $h$ is locally increasing or decreasing, and thus, if $\mu_{\text{diff}}^{+}$ or $\mu_{\text{diff}}^{-}$ has to be used. An iterative solver can possibly be used, but the discontinuity may hinder the solver and may lead to a not converging sequence. To fix this, one can create a smooth function $\mu_{\text{diff}}$, e.g., by employing a sigmoid-like transition between $\mu_{\text{diff}}^{+}$ and $\mu_{\text{diff}}^{-}$. Unfortunately, this still increases the sensitivity of the problem, and thus can lead to a significantly reduced step size. Moreover, if the step sizes are chosen too small, $\mu_{\text{diff}}$ might use the artificial values of the transition zone for a longer period yielding inappropriate overall simulation results. For these reasons, we have not pursued this concept any further.

In our current approach, $\mu_{\text{diff}}^{+}$ or $\mu_{\text{diff}}^{-}$ is used if the $h$ value was in- or decreased in the last time step, respectively. Hence, this approach can only react to a change of $\operatorname{sgn}(\frac{dh}{dt})$ with a delay of one time step. In a simulation, $\mu_{\text{diff}}$ needs to be computed on a discrete set of points (for each element) and we need to store the data from the previous time step. We globally initialize $\mu_{\text{diff}} = \frac{1}{2}(\mu_{\text{diff}}^{+} + \mu_{\text{diff}}^{-})$, and then, update $\mu_{\text{diff}}$ element-wise after each calculation by

$$\mu_{\text{diff}} = \begin{cases} \mu_{\text{diff}}^{+} & \text{if } h_{\text{new}} > h_{\text{old}}, \\ \mu_{\text{diff}}^{-} & \text{if } h_{\text{new}} < h_{\text{old}}. \end{cases} \tag{8}$$

The advantage of this procedure is that $\mu_{\text{diff}}$ is locally, per time step fixed. Thus, it does not hinder the solver in any way and it allows usage of non-iterative solvers.

b) Tellinen's model does not calculate $\mu$, $b$ or $h$. For a given state $(h,b)$ and direction $\operatorname{sgn}(\frac{dh}{dt})$, it outputs the change of $b$, i.e., $\mu_{\text{diff}} = \frac{db}{dh}$. To obtain new field values, we suggest a linear approach

$$b_{\text{new}} = b_{\text{old}} + \mu_{\text{diff}}(h_{\text{new}} - h_{\text{old}}) \qquad \text{or} \qquad h_{\text{new}} = h_{\text{old}} + \frac{1}{\mu_{\text{diff}}}(b_{\text{new}} - b_{\text{old}}). \tag{9}$$

For example, for the magnetoquasistatic approximation of Maxwell's equations in terms of the magnetic vector potential $\vec{A}$, one obtains the curl-curl equation:

$$\sigma \frac{d\vec{A}}{dt} + \nabla \times \left( \frac{1}{\mu} (\nabla \times \vec{A}) \right) = \vec{J} \tag{10}$$

with conductivity $\sigma$, applied current $\vec{J}$ and $\vec{B} = \nabla \times \vec{A}$. Using (9), this yields

$$\sigma \frac{d\vec{A}}{dt} + \nabla \times \left( \frac{1}{\mu_{\text{diff}}} (\nabla \times \vec{A}) \right) = \vec{J} + \nabla \times \left( \frac{1}{\mu_{\text{diff}}} \vec{B}_{\text{old}} - \vec{H}_{\text{old}} \right). \tag{11}$$

Here, the incorporation of Tellinen's model into (10) is simple. Since the left-hand side remains the same, the solvability should not be worsened.

**Possible further improvements.** Tellinen's model needs very few inputs, namely $B^+_{\text{sat}}$ and its derivative. Thus a combination with other models as preprocessor is possible if the inputs are computable. For example in [4], the Jiles-Atherton model [7] is used to generate $B^+_{\text{sat}}$. Thus, the Tellinen model can be easily compared and combined with other models as long as $B^+_{\text{sat}}$ is shared.

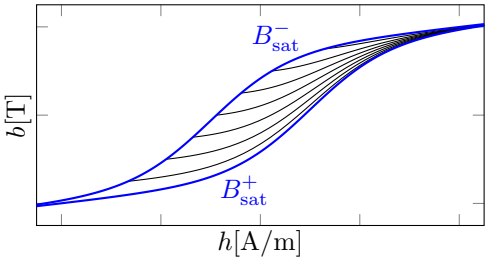


Figure 2: An example of saturation curves $B^+_{\text{sat}}$, $B^-_{\text{sat}}$ and intermediate curves, so-called first-order reversal curves.

Moreover, it is possible to add the data of intermediate first-order reversal curves to the measured saturation curves $B^+_{\text{sat}}$ and $B^-_{\text{sat}}$, see Fig 2. Then, the linear interpolation for a given operation point $(b,h)$ can be restricted to the two adjacent curves. This approach is necessary if the material exhibits a pronounced non-linear behavior along $h=$const and $B^+_{\text{sat}}(h) \le b \le B^-_{\text{sat}}(h)$. The complexity of this approach is low and the additional computation cost at runtime is small.

These ideas can be as well applied to the thermal extension developed next.

## 3 Thermal Extension of Hysteresis

Using the same concepts as Tellinen, we develop a thermal extension by defining the partial derivatives $\frac{\partial b}{\partial T}$ dependent on the $\operatorname{sgn}(\partial T)$. Again, a physical motivation is given based on measured saturation boundary and linear interpolation for the intermediate points. Ultimately, the extended model shall approximate the material behaviour in terms of $b$ if a current state $(h,b,T)$ is changed w.r.t. to $h$ and $T$.

**Input data.** Let $B^+_{\text{sat}} = B^+_{\text{sat}}(h,T) \in C^1$ be a function that defines the saturation value of $b$ for a given field strength $h$ and temperature $T$ in the case $h$ monotonously increased from $h \ll 0$ to $h \gg 0$. Analogously to (3), the derivative w.r.t. $h$ has to be bounded from below:

$$\frac{\partial}{\partial h} B^+_{\text{sat}}(h,T) \ge \mu_0\,, \qquad \lim_{|h|\to\infty} \tfrac{\partial}{\partial h} B^+_{\text{sat}}(h,T) = \mu_0\,.$$

As in (2), $B^-_{\text{sat}}(h,T)$ can be defined by symmetry and it shall satisfy

$$B^+_{\text{sat}}(h,T) < B^-_{\text{sat}}(h,T) := -B^+_{\text{sat}}(-h,T), \quad \lim_{|h|\to\infty} \left(B^-_{\text{sat}}(h,T) - B^+_{\text{sat}}(h,T)\right) = 0.$$

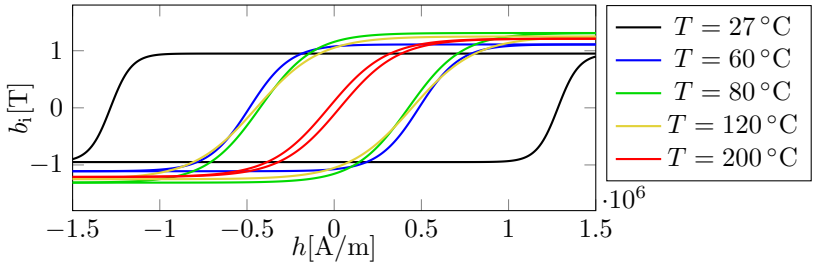


Figure 3: Sample curves depicting the intrinsic induction $b_\mathrm{i}$ versus the magnetic field strength $h$ for various temperatures. These curves are based upon measurements of NdFeB magnets [1], but simplified for demonstration.

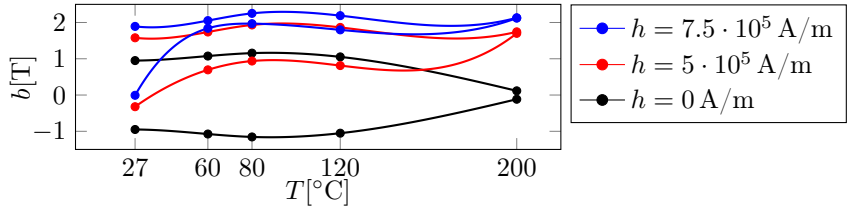


Figure 4: Shown are $B^+_\mathrm{sat}(h,T)$ and $B^-_\mathrm{sat}(h,T)$ for fixed values of $h$. The same dataset as in Fig. 3 is used. The interpolation is based on a spline approach.

Here, the valid states (4) become

$$I_\mathrm{T} = \left\{(h,b,T) \in \mathbb{R}^3 \,\middle|\, B^+_\mathrm{sat}(h,T) \le b \le B^-_\mathrm{sat}(h,T)\right\}.$$

One possibility to define such $B^+_\mathrm{sat}(h,T)$ is to interpolate several $b/h$-curves of different temperatures. For fixed $h$, $B^\pm_\mathrm{sat}(h,\cdot)$ might have no monotonicity, see Fig. 4.

**Physical motivation and computation.** For a fixed temperature $T$ and varying $h$, the non-thermal Tellinen model is used by just replacing $B^\pm_\mathrm{sat}(h)$ by $B^\pm_\mathrm{sat}(h,T)$. We will now discuss the situation of fixed $h$ and varying $T$. The combination of both, defines the temperature dependent Tellinen model. We remark that no solution, starting from a valid point $(h,b,T) \in I_\mathrm{T}$, may leave $I_\mathrm{T}$. Now, given surfaces $B^\pm_\mathrm{sat}(h,T)$ and for any $(h,b,T) \in I_\mathrm{T}$, $\lambda$ can be calculated analogously to (5). Firstly, for an increasing temperature $\partial T > 0$, it can be argued that the material's molecules can move and rotate more freely. Therefore, they can follow the measured values on the boundaries as good as possible. Hence, we define

$$\frac{\partial b}{\partial T} = \lambda \frac{\partial}{\partial T} B^+_\mathrm{sat}(h,T) + (1-\lambda)\frac{\partial}{\partial T} B^-_\mathrm{sat}(h,T) \quad \text{for } \partial T > 0. \tag{12}$$

Secondly, reducing the temperature, the ability of the molecules to rearranging themselves is decreased. They tend to freeze and try to retain their current state.

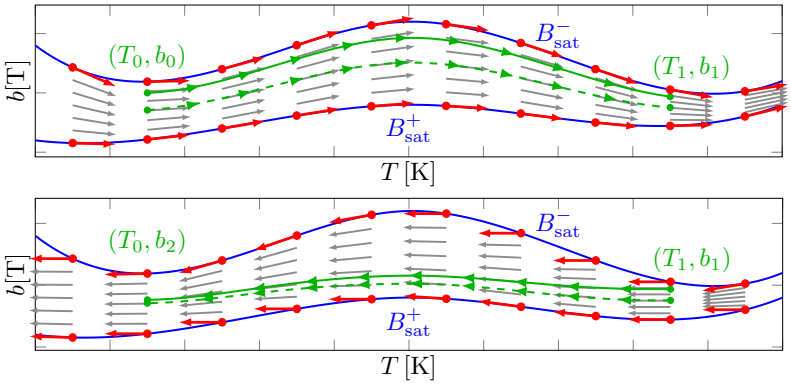


Figure 5: For constant $h$, exemplary bounding saturation curves $B^{\pm}_{\mathrm{sat}}(h,T)$ are shown. Arrows represent the assigned values of $\frac{\partial b}{\partial T}$ for an increasing (upper plot) and decreasing (lower plot) temperature $T$. The inner solid path represent the solution of $b$ starting at $(T_0, b_0)$, and increasing temperature to $T_1$ (upper) and going back to $T_0$ (lower). Generally, $b_0 \neq b_2$. The dashed curve shows a stable loop, where start and end point coincide.

Therefore, for $\partial T < 0$, we like to assign $\frac{\partial b}{\partial T} = 0$. However, there are cases where this will lead to values of $b$ outside to the set $I_{\mathrm{T}}$. To handle this, we assigns the value of zero whenever possible. Otherwise, the measured value on the boundary are used, such that $I_{\mathrm{T}}$ can not be leaved. This reads: (see Fig. 5)

$$\frac{\partial b}{\partial T} = \lambda \min\left(\tfrac{\partial}{\partial T} B^+_{\mathrm{sat}}(h,T), 0\right) + (1-\lambda)\max\left(\tfrac{\partial}{\partial T} B^-_{\mathrm{sat}}(h,T), 0\right) \text{ for } \partial T < 0\,. \quad (13)$$

**Properties.** The definition of the partial derivatives (12-13) ensures that an analytically solution starting in $I_{\mathrm{T}}$ always stays within $I_{\mathrm{T}}$. Keeping $h$ constant and increasing $T$, (12) will change a state from $(T_0, b_0)$ to $(T_1, b_1)$. But reducing $T$ back to $T_0$ via (13), one generally ends up in $(T_0, b_2)$ with $b_0 \neq b_2$, see Fig. 5. Thus, this model reflects a non-reversibility behavior. However, also stable loops exist. It can be shown that, for a given interval $[T_0, T_1]$, there is exactly one stable loop, such that $b_0 = b_2$ holds, or all loops are stable. If a loop is unstable, it convergences against a stable loop if $T$ is periodically alternated between $T_0$ and $T_1$. The situation that all loops with $B^+_{\mathrm{sat}} \leq b_0 \leq B^-_{\mathrm{sat}}$ are stable, can only occur if $\frac{\partial}{\partial T} B^+_{\mathrm{sat}}(h,T) \leq 0$ and $\frac{\partial}{\partial T} B^-_{\mathrm{sat}}(h,T) \geq 0$ for all $T \in [T_0, T_1]$. In this special case, (12) and (13) are equal and a reversible progress is given. For $h = 0$ and uniqueness of the stable curve, this stable curve is defined by $b = 0$ for all $T$. Thus, any valid $b_0$ will lead to a gradual depolarization of the material.

**Simulation.** In time domain, temperature is often slower evolving than the magnetic fields. Therefore, we allow that the temperature values are updated only in

every $k$-th time step; elsewhere, they are assumed to be constant. Now, to implement the thermal extension, we perform an additional adjustment of the $b$ field in every $k$-th time step. This can be realized by the following linear approach

$$b_{\text{new}} = b_{\text{old}} + \frac{\partial b}{\partial T} \cdot (T_{\text{new}} - T_{\text{old}}), \tag{14}$$

where $\frac{\partial b}{\partial T}$ is given by (12) or (13). Overall, it is ensured that an analytical solution stays in $\in I_{\text{T}}$. This approach enables multirate simulation (for $k > 1$).

## 4 Conclusion and Outlook

A thermal extension of Tellinen's hysteresis model was proposed and based of the same ideas as given in the original version. The thermal model describes $b$ in terms of $h$ and $T$. It reflects fundamental, physical phenomena, e.g., the irreversibility and depolarization. Currently, we investigate the computation of magnetic losses based on the extended thermal model. A comparison to other thermal models is also a pending task.

## References


[1] Ghezelbash, M., Darbani, S., Majd, A., Ghasemi, A.: Temperature Dependence of Magnetic Hysteresis Loop of NdFeB with Uniaxial Anisotropy by LIBS Technique. J. Supercond. Nov. Magn., **30**, 1893–1898 (2017)

[2] Raghunathan, A., Melikhov, Y., Snyder, J., Jiles, D.: Theoretical Model of Temperature Dependence of Hysteresis Based on Mean Field Theory. IEEE Trans. on Magn., **46**, 1507-1510 (2010)

[3] Sixdenier, F., Messal, O., Hilal, A., Martin, C., Raulet, M., Scorretti, R.: Temperature-Dependent Extension of a Static Hysteresis Model. IEEE Trans. Magn., **52**, 1-4 (2016)

[4] Steentjes, S., Hameyer, K., Dolinar, D., Petrun, M.: Iron-Loss and Magnetic Hysteresis Under Arbitrary Waveforms in NO Electrical Steel: A Comparative Study of Hysteresis Models. IEEE Trans. Ind. Electron., **64**, 2511-2521 (2017)

[5] Tellinen, J.: A simple scalar model for magnetic hysteresis. IEEE Trans. Magn., **34**, 2200-2206 (1998)

[6] Güntzel, U., Westerholt, K., Methfessel, S.: Temperature dependence of the magnetic hysteresis properties of some metglasses between 4.2 and 300K. J. Magn. Magn. Mater., **38**, 294-300 (1983)

[7] Jiles, D. C., Atherton, D. L.: Theory of ferromagnetic hysteresis. J. Appl. Phys., **55**, 2115-2120 (1984)

[8] Preisach, F.: Über die magnetische Nachwirkung. Zeitschrift für Physik, **94**, 277-302 (1935)

[9] Bobbio, S., Milano, G., Serpico, C., Visone, C.: Models of magnetic hysteresis based on play and stop hysterons. IEEE Trans. Magn., **33**, 4417-4426 (1997)